A Comparison Between Quadrotor Flight Configurations

Robert Niemiec
Graduate Student and NDSEG Fellow
Rensselaer Polytechnic Institute
Troy, New York, USA

Farhan Gandhi
Redfern Chair in Aerospace Engineering
Rensselaer Polytechnic Institute
Troy, New York, USA

ABSTRACT

This paper compares a quadcopter operating in the plus and cross configurations. Using mutli-rotor controls (Ω_0 collective, Ω_P pitch, Ω_R roll, and Ω_Y yaw control), the plus-configuration generates a yaw moment when a pitch or roll control input is introduced; but for the cross-configuration, pitch and roll control is decoupled from yaw. While the collective control, pitch attitude, and power requirement versus flight speed are identical for both configurations, in forward flight the plus-configuration requires a larger pitch control input since it uses only two rotors, and a compensatory yaw control input. Quadcopters display two oscillatory modes in hover, a longitudinal phugoid mode (coupling longitudinal translation and pitch) and a lateral phugoid mode (coupling lateral translation and roll). Both these modes are stable and their poles are coincident in hover. In forward flight, these modes separate, and the frequency and damping of both modes increases. The nature of the lateral phugoid mode in forward flight is very similar to hover, but the longitudinal phugoid mode begins to include altitude changes (in addition to longitudinal translation and pitch attitude). Over a certain airspeed range, a couple of real poles (corresponding to heave and pitch subsidence) combine to result in an oscillatory short-period mode. No significant difference is seen in the autonomous flight dynamic characteriscs (pole locations) between the plus- and cross-configurations. A comparison of the control authority available between the plus- and cross-configuration quadcopters shows that while collective and yaw control authority is identical, pitch and roll control authority is up to about 30% greater for the cross-configuration since all four (as opposed to only two) rotors are used.

NOTATION

a	Rotor Thrust Proportionality Constant – kg m
A	Linearized Aircraft Plant Model
$\bar{A}$	Reduced Aircraft Plant Model
A_{11}	Rigid Body Stability Derivatives
A_{12}	Rigid Body - Inflow Stability Derivatives
A_{21}	Inflow - Rigid Body Stability Derivatives
A_{22}	Inflow Stability Derivatives
b	Rotor Torque Proportionality Constant – kg m^2
B	Linearized Control Derivatives
$\bar{B}$	Reduced Control Derivatives
B_1	Rigid Body Control Derivatives
B_2	Inflow Control Derivatives
CCW	Counter-clockwise
CW	Clockwise
C_Q	Torque Coefficient
C_T	Thrust Coefficient
l	Rotor Boom Length – m
L	Aircraft Rolling Moment – Nm
L_v	Roll Acceleration from Lateral Translation – $\frac{\text{rad}}{\text{m s}}$
L_p	Roll Acceleration from Roll Rate – $\frac{\text{rad}}{\text{s}}$
L_ϕ	Roll Acceleration from Roll Attitude – $\frac{\text{rad}}{\text{s}^2}$
L_{Ω_R}	Roll Acceleration from Diff. Roll RPM– $\frac{1}{\text{s}}$
M	Aircraft Pitching Moment – Nm
M_u	Pitching Acceleration from Longitudinal Translation $\frac{\text{rad}}{\text{m s}}$
M_q	Pitch Acceleration from Pitch Rate – $\frac{\text{rad}}{\text{s}}$
M_θ	Pitch Acceleration from Pitch Attitude – $\frac{\text{rad}}{\text{s}^2}$
M_{Ω_P}	Pitch Acceleration from Diff. Pitch RPM– $\frac{1}{\text{s}}$
N_r	Yaw Acceleration from Yaw Rate – $\frac{\text{rad}}{\text{s}}$
N_{Ω_Y}	Yaw Acceleration from Diff. Yaw RPM– $\frac{1}{\text{s}}$
p	Aircraft Roll Rate – $\frac{\text{rad}}{\text{s}}$
q	Aircraft Pitch Rate – $\frac{\text{rad}}{\text{s}}$
r	Aircraft Yaw Rate – $\frac{\text{rad}}{\text{s}}$
RPM	Rotor Speed in Revolutions per Minute
T	Aircraft Total Thrust – N
T_i	Individual Rotor Thrust – N
u	Aircraft Longitudinal Velocity – $\frac{\text{m}}{\text{s}}$
$\vec{u}$	Control Vector
v	Aircraft Lateral Velocity – $\frac{\text{m}}{\text{s}}$
w	Aircraft Heave Velocity – $\frac{\text{m}}{\text{s}}$
X_u	Longitudinal Acceleration from Longitudinal Velocity – $\frac{1}{\text{s}}$
X_θ	Longitudinal Acceleration from Pitch Attitude – $\frac{\text{m}}{\text{s}^2}$
Y_v	Lateral Acceleration from Lateral Velocity – $\frac{1}{\text{s}}$
Y_ϕ	Lateral Acceleration from Roll Attitude – $\frac{\text{m}}{\text{s}^2}$
Z_w	Heave Acceleration from Heave Velocity – $\frac{1}{\text{s}}$
Z_{Ω_0}	Heave Acceleration from Collective Control– $\frac{\text{m}}{\text{s}}$
ϕ	Aircraft Roll Attitude

Presented at the 42nd European Rotorcraft Forum, Lille, France, September 5–8, 2016.

θ Aircraft Pitch Attitude
ψ Aircraft Heading
Ψ_i Azimuthal Location of Rotor i
τ_i Rotor i Torque – Nm
Ω_0 Collective Control – RPM
Ω_P Pitch Control – RPM
Ω_R Roll Control – RPM
Ω_Y Yaw Control – RPM
Ω_N, Ω_E
Ω_S, Ω_W Individual rotor speeds in plus-configuration – RPM
Ω_{NE}, Ω_{NW}
Ω_{SW}, Ω_{SE} Individual rotor speeds in cross-configuration – RPM

INTRODUCTION

Multirotor aircraft are a newly popular platform for use in small UAVs. In lieu of a large main rotor controlled with collective and cyclic pitch inputs, they use multiple fixed-pitch, variable RPM propellers to produce thrust and moments necessary for controlled flight. Their simplicity and ease of use has made them popular among hobbyists and researchers alike. Additionally, there has been interest in multirotor UAVs in applications such as law enforcement, border and homeland security and defense, as well as commercial interest for applications like package delivery or aerial photography.

The simplest fully controllable multirotor aircraft is the quadcopter, which uses four rotors connected to the fuselage via booms, generally arranged in a square pattern. The quadcopter features two sets of counter-rotating rotors, arranged such that adjacent rotors spin in opposite directions (Fig. 1). On a quadcopter, there are two common ways to fly. The first is a "plus" configuration, in which a single rotor leads the aircraft (Fig. 1(a)). The other is the "cross" configuration, where two rotors lead the aircraft (Fig. 1(b)).

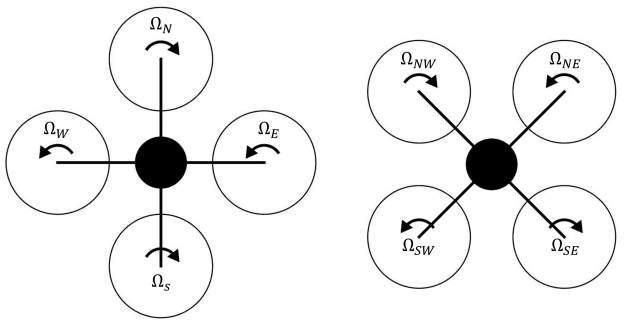

(a) Plus Configuration (b) Cross Configuration

Fig. 1: Quadrotor Flight Configurations

Both types of quadcopter flight configurations have been used in previous work. Pounds et al. designed and modeled a cross-configuration quadcopter across a series of papers dating back to 2002 ((Ref. 1) – (Ref. 4)). A quadcopter developed by Haviland et al. (Ref. 5) for the American Helicopter Society Student MAV design competition also used the cross-configuration. In 2016, Avera et al. (Ref. 6) assessed a cross-configuration quadcopter with overlapping rotors for use in densely populated urban environments.

The plus-configuration quadcopter has also seen wide use. The STARMAC II, developed at Stanford University (Ref. 7), (Ref. 8), is a plus-type quadcopter. Bouabdallah and Seigwart (Ref. 9) and Erginer and Altuğ (Ref. 10) both developed models and controllers for plus-type quadcopters. More recently, Mueller and D'Andrea developed a controller to stabilize a plus-type quadcopter despite the loss of rotor power (Ref. 11). Mulgaonkar et al. developed a plus-type quadcopter swarm for formation flight (Ref. 12). Previous work by the authors developed a dynamic simulation of a plus-type quadcopter (Ref. 13), and used it to assess the effects of the inflow model on the aircraft trim and flight dynamics.

QUADCOPTER MULTI-ROTOR CONTROLS

The quadcopter has four control inputs, corresponding to the rotational speed of each of its rotors. While it is valid to command the speed of each rotor individually, this produces a highly coupled response. For example, when the speed of the front rotor (Ω_N in Fig. 1(a)) of a plus-type quadcopter is changed, the aircraft experiences a net change in the thrust, pitching moment, and yawing torque in hover; in forward flight, it will also produce a rolling moment.

However, a set of multi-rotor controls exists that are more effective at decoupling the aircraft response. These controls include a collective control (Fig. 2), pitch control (Fig. 3), roll control (Fig. 4), and yaw control (Fig. 5). Collective Control increases the speed of all four rotors simultaneously, increasing the thrust of the aircraft without producing moments. Pitch control increases RPM on the front rotor(s), while decreasing RPM on the aft rotor(s), producing a nose-up pitching moment. Similarly, roll control increases RPM on the left rotor(s), while decreasing RPM on the right rotor(s) to produce a roll-right moment. Finally, yaw control increases the speed of the CCW rotors, while decreasing the speed of the CW rotors, producing a nose-right torque. An important distinction between the plus- and cross-type quadcopters is that when producing a pitching or rolling moment, the cross-type uses all four rotors, as opposed to the plus-type's use of only two rotors. On the other hand, for equal boom length, the pitching/rolling moment arm is 30% shorter on the cross-type quadcopter than on the plus-type, partially mitigating the advantage in control authority.

From these four multi-rotor controls, the speeds of the individual rotors can be determined. For the plus-configuration, the individual rotor speeds are defined as a function of Ω_0, Ω_P, Ω_R, and Ω_Y in equation 1, and the same for the cross-configuration in equation 2.

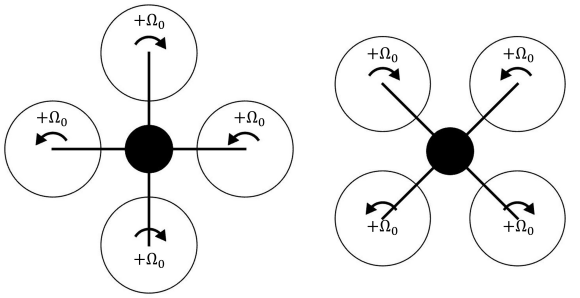

(a) Plus Configuration (b) Cross Configuration

Fig. 2: Collective Control (Ω_0)

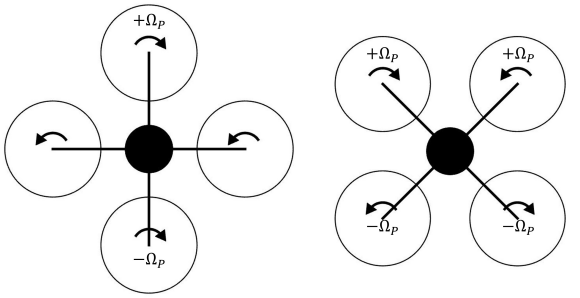

(a) Plus Configuration (b) Cross Configuration

Fig. 3: Pitch Control (Ω_P)

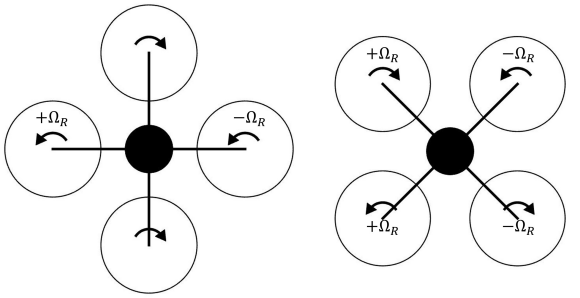

(a) Plus Configuration (b) Cross Configuration

Fig. 4: Roll Control (Ω_R)

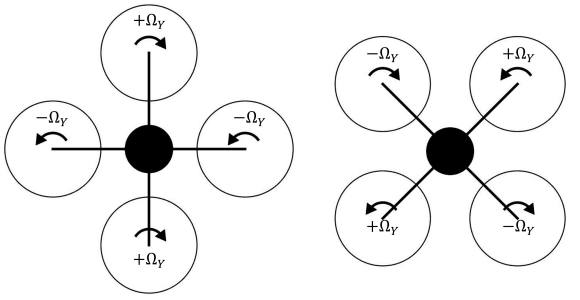

(a) Plus Configuration (b) Cross Configuration

Fig. 5: Yaw Control (Ω_Y)

The columns of the matrices on the right hand side in Eqs. 1 and 2 represent the collective, pitch, roll and yaw control modes for the plus and cross-configurations, respectively. Although these control modes are orthogonal to each other for both configurations, their ability to affect only a single axis merits further discussion. For both the plus and the cross-configurations, the collective mode, associated with control Ω_0 affects only the generated thrust and does not generate any pitch, roll, or yaw moments.

$$\begin{bmatrix} \Omega_N \\ \Omega_W \\ \Omega_S \\ \Omega_E \end{bmatrix} = \begin{bmatrix} 1 & 1 & 0 & 1 \\ 1 & 0 & 1 & -1 \\ 1 & -1 & 0 & 1 \\ 1 & 0 & -1 & -1 \end{bmatrix} \begin{bmatrix} \Omega_0 \\ \Omega_P \\ \Omega_R \\ \Omega_Y \end{bmatrix} \tag{1}$$

$$\begin{bmatrix} \Omega_{NE} \\ \Omega_{NW} \\ \Omega_{SW} \\ \Omega_{SE} \end{bmatrix} = \begin{bmatrix} 1 & 1 & -1 & 1 \\ 1 & 1 & 1 & -1 \\ 1 & -1 & 1 & 1 \\ 1 & -1 & -1 & -1 \end{bmatrix} \begin{bmatrix} \Omega_0 \\ \Omega_P \\ \Omega_R \\ \Omega_Y \end{bmatrix} \tag{2}$$

For the cross-configuration, consider the pitch mode, (associated with Ω_P), where the two front rotors speed up and the two rear rotors slow down to generate a nose-up pitching moment. Of the two front rotors speeding up, one of them rotates in the CW direction and the other in the CCW direction, and the torque generated cancels out. The same is true of the rear rotors slowing down. Thus, pitch control does not introduce a net yaw moment on the cross-configuration quadcopter. Similarly, the two left rotors speed up and the two right rotors slow down to generate a roll-right moment. Of the two left rotors speeding up, since one of them is a CW-spinning and the other is a CCW-spinning rotor, their torques cancel. The same is true for the two right rotors slowing down, so, as in the case of pitch mode, roll control, associated with Ω_R, does not introduce a net yaw moment on the cross-configuration quadcopter.

The plus-configuration quadcopter differs in this regard. The pitch control mode speeds up the single front rotor and slows down the single rear rotor to generate a nose-up pitching moment. Since torque does not vary linearly with RPM (variation is nominally quadratic), the increase in torque of the CCW spinning front rotor does not identically cancel with the torque reduction of the CCW spinning rear rotor, resulting in a net yaw moment on the plus-configuration quadcopter, requiring compensation with a yaw control input. Similarly, the roll control mode speeds up the single left rotor and slows down the single right rotor to generate a roll-right moment on the plus-configuration quadcopter. The torque increase in the CW spinning right rotor does not identically cancel with the torque reduction of the CW spinning right rotor, so as in the case of the pitch control mode, the roll control mode results in a net yaw moment on the plus-configuration quadcopter, which would require compensation by a yaw control input.

For both the plus- as well as the cross-configuration quadcopters, the yaw mode, associated with Ω_Y, does not generate any pitch or roll moments on the aircraft. On the other hand,

for both configurations, the pitch, roll, and yaw control modes result in a small net changes in thrust (nominally quadratic), and require compensatory collective control input. This is related to the rotor thrust not varying linearly (variation is nominally quadratic) with rotor speed, so the increase in thrust of speeding up rotors does not cancel identically with reduction in thrust from rotors slowing down by the same amount.

Of course, if the inputs were infinitesimally small, these higher order effects become negligible, and, in the limit, go to zero. It should be noted that orthogonality of modes is a concept associated with linear systems, so even though the control modes in Eqs. 1 and 2 are orthogonal, the axes are not entirely decoupled due to the nonlinear response of individual rotors to change in RPM, and by extension the nonlinear response of the quadcopter to finite control inputs. That having been said, there remains a clear distinction between the cross and plus-configuration quadcopters in that pitch and roll control modes on the cross-configuration are decoupled from yaw, while pitch and roll control modes on a plus-configuration introduce yawing moments on the aircraft.

MODELING

To assess the behavior of the quadcopters, a dynamic simulation is constructed. The simulation determines accelerations by summing the forces acting on the quadcopter. These forces include gravity, fuselage drag (modeled as a cylinder), and rotor forces/moments. The rotor forces and moments are obtained using Blade Element Theory with a 3x4 (10 state) Peters-He dynamic wake (Ref. 14) to calculate inflow velocity. The Peters-He model ties the inflow distribution to the thrust distribution, and since each rotor is generally operating at its own unique speed, each rotor needs its own set of inflow states, bringing the total number of inflow states to 40. Additionally, since the rotors are modeled as rigid, aerodynamic forces also produce moments at the rotor hub that are transferred to the aircraft.

This simulation is based on a 2kg gross weight helicopter based on the AeroQuad Cyclone ARF kit (Fig. 6), which can be flown either in the plus- or cross-configurations. The AeroQuad Cyclone has four 12 inch diameter rotors, and its geometry is described in Table 1.

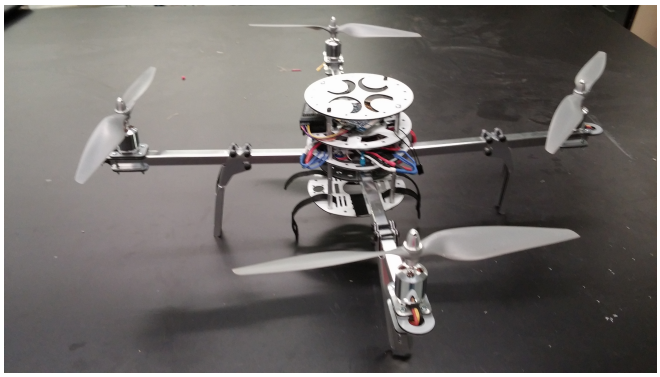

Fig. 6: AeroQuad Cyclone ARF kit

Table 1: Blade Geometry

Parameter	Value
Rotor Radius	0.1524m
Root Pitch	21.5°
Tip Pitch	11.1°
Root Chord	0.031 m
Tip Chord	0.012 m
Boom length	0.3048m
Motor/Rotor mass	0.060kg each

Trimming the aircraft involves solving for the quadcopter controls (Ω_0, Ω_P, Ω_R, and Ω_Y) and the roll and pitch attitudes that drive all linear and angular accelerations to zero. Additionally, the inflow states are all solved such that their first derivatives are zero.

After trimming the aircraft, the nonlinear dynamic model is numerically linearized about a trim condition in order to assess the flight dynamics of the quadcopter. This linear model takes the form of equation 3, where the matrix A represents the plant model whose entries are the sensitivity derivatives of the model. The matrix B is a control sensitivity matrix. The full system includes 12 aircraft states (3 positions, 3 attitudes, and derivatives), as well as 40 inflow states (10 per rotor), for a total of 52 states, and 4 control inputs. The states x and controls u are defined as changes from a trim condition.

$$\dot{\vec{x}} = A\vec{x} + B\vec{u} \tag{3}$$

where

$$\vec{x} = \begin{bmatrix} x & y & z & \phi & \theta & \psi & u & v & w & p & q & r & \vec{\lambda} \end{bmatrix}^T$$
$$\vec{u} = \begin{bmatrix} \Delta\Omega_0 & \Delta\Omega_P & \Delta\Omega_R & \Delta\Omega_Y \end{bmatrix}^T$$

where $\vec{\lambda}$ represents the inflow states.

The autonomous behavior of the aircraft is considered by setting $u = \bar{0}$, so the system reduces to equation 4. In this form, an eigen analysis on the matrix A will yield information about the dynamic modes of the aircraft.

$$\dot{\vec{x}} = A\vec{x} \tag{4}$$

In the Peters-He model, the dynamics of the inflow occur on the same time scale as the speed of rotor revolution. As such, static condensation can be used to reduce the size of the problem. The states are partitioned into two groups, one containing the body states, and the other containing the inflow states. Equation 3 then becomes

$$\begin{aligned} \dot{\vec{x}_1} &= A_{11}\vec{x_1} + A_{12}\vec{x_2} + B_1\vec{u} \\ \dot{\vec{x}_2} &= A_{21}\vec{x_1} + A_{22}\vec{x_2} + B_2\vec{u} \end{aligned} \tag{5}$$

where x_1 represents the body states, and the x_2 describes the inflow states. Because the poles of the inflow modes are very

stable, $\dot{x_2}$ can be taken to be zero. Solving the resulting equation for x_2 and substituting yields the reduced model, equation 6.

$$\begin{aligned}\dot{\vec{x_1}} &= (A_{11} - A_{12}A_{22}^{-1}A_{21})\vec{x_1} + (B_1 - A_{12}A_{22}^{-1}B_2)\vec{u} \\ &= \bar{A}\vec{x_1} + \bar{B}\vec{u}\end{aligned} \tag{6}$$

$$\vec{x_1} = \begin{bmatrix} x & y & z & \phi & \theta & \psi & u & v & w & p & q & r \end{bmatrix}^T$$

where, in hover, $\bar{A}$ takes the form

$$\bar{A} = \begin{bmatrix} 0 & 0 & 0 & 0 & 0 & 0 & 1 & 0 & 0 & 0 & 0 & 0 \\ 0 & 0 & 0 & 0 & 0 & 0 & 0 & 1 & 0 & 0 & 0 & 0 \\ 0 & 0 & 0 & 0 & 0 & 0 & 0 & 0 & 1 & 0 & 0 & 0 \\ 0 & 0 & 0 & 0 & 0 & 0 & 0 & 0 & 0 & 1 & 0 & 0 \\ 0 & 0 & 0 & 0 & 0 & 0 & 0 & 0 & 0 & 0 & 1 & 0 \\ 0 & 0 & 0 & 0 & 0 & 0 & 0 & 0 & 0 & 0 & 0 & 1 \\ 0 & 0 & 0 & 0 & X_\theta & 0 & X_u & 0 & 0 & 0 & 0 & 0 \\ 0 & 0 & 0 & Y_\phi & 0 & 0 & 0 & Y_v & 0 & 0 & 0 & 0 \\ 0 & 0 & 0 & 0 & 0 & 0 & 0 & 0 & Z_w & 0 & 0 & 0 \\ 0 & 0 & 0 & L_\phi & 0 & 0 & 0 & L_v & 0 & L_p & 0 & 0 \\ 0 & 0 & 0 & 0 & M_\theta & 0 & M_u & 0 & 0 & 0 & M_q & 0 \\ 0 & 0 & 0 & 0 & 0 & 0 & 0 & 0 & 0 & 0 & 0 & N_r \end{bmatrix}$$

where each entry is a stability derivative with respect to the state denoted in the subscript.

TRIM RESULTS

Fig. 7 shows the quadcopter pitch attitude versus its forward speed. As the speed increases, the quadcopter increasingly needs to vector its thrust forward to overcome drag. Without blade flapping, the only means by which the quadcopter can do so is to pitch the entire aircraft nose-down. The aircraft drag is unaffected by the configuration of the quadcopter because the fuselage is radially symmetric, so the required pitch attitude is the same between the plus and cross-configurations. Similarly, the collective control requirements are identical between the plus and cross-configurations (Fig. 8), since they also have the same weight.

In forward flight, each rotor produces a nose-up pitching moment. This is because the longitudinal inflow distribution causes in increase in lift on the front of each rotor, and a reduction on the aft (Fig. 9). In order to maintain trim, a steady pitch control (Ω_P) must be applied (Fig. 10). It can be shown that with a lower-order model (i.e. $T, \tau \propto \Omega^2$) that the plus-configuration needs $\sqrt{2}$ times the pitch input as the cross-configuration (compare eqns. 12 and 13). This is because the cross-configuration uses all four rotors to produce a pitching moment, as opposed to the plus-configuration's two (Fig. 3).

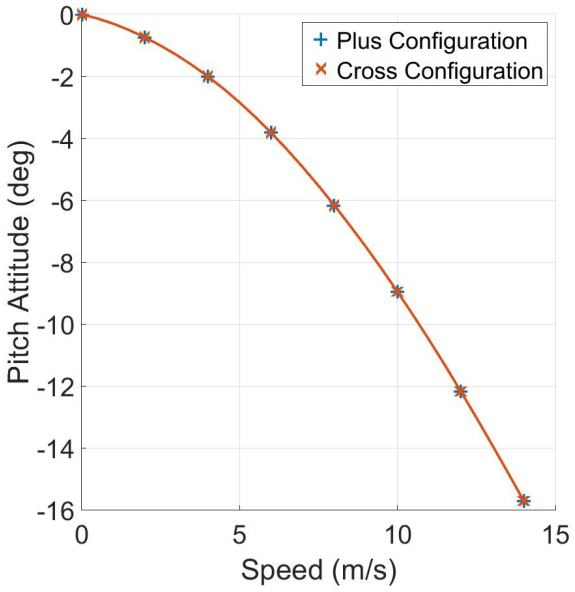

Fig. 7: Pitch Attitude versus Flight Speed

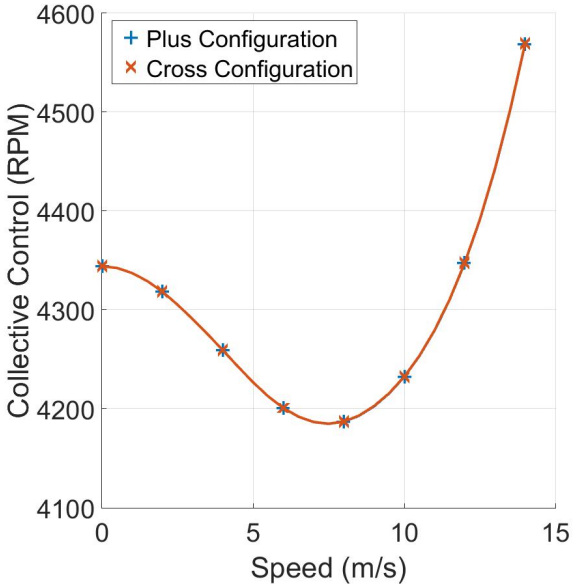

Fig. 8: Collective Control versus Flight Speed

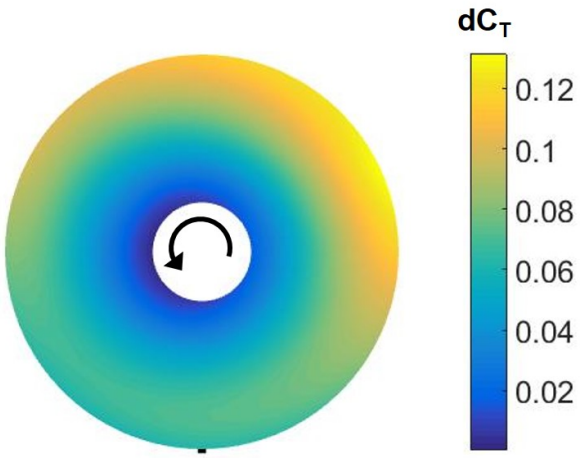

Fig. 9: Thrust Distribution over Front Rotor (Plus Configuration) at 5 m/s flight speed

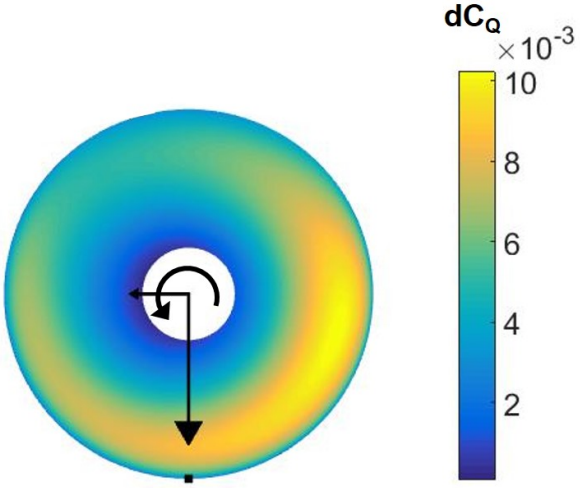

Fig. 11: Torque Distrubution on front rotor (Plus Configuration) at 5 m/s flight speed

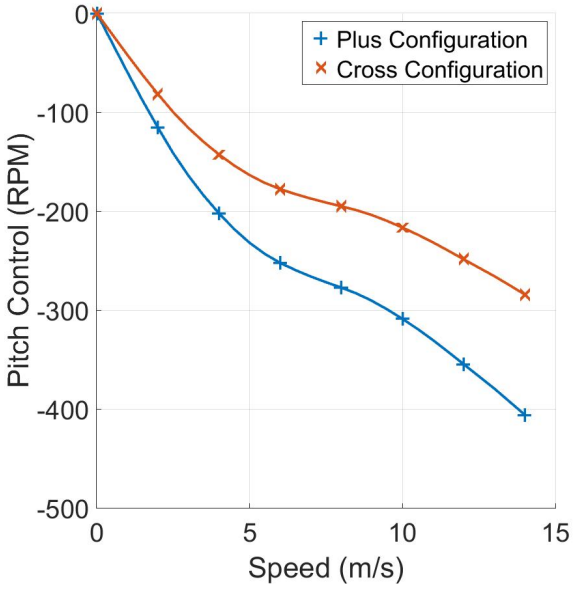

Fig. 10: Pitch Control versus Flight Speed

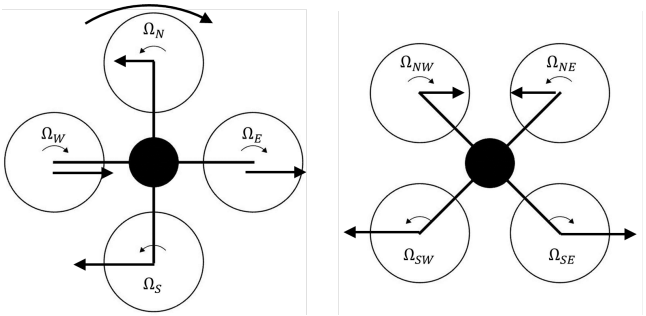

(a) Plus Configuration (b) Cross Configuration

Fig. 12: Side forces on aircraft

Additionally, the longitudinal inflow distribution causes an increase in blade drag on the aft of the rotor disk, relative to the front (Fig. 11). As a result, the rotor, spinning counter-clockwise, produces a net side force to the left. The magnitude of this side force is proportional to the integrated thrust generated by the rotor, and the direction is defined by the spin direction of the rotor (i.e. a rotor spinning clockwise will produce a side force to the right). Each rotor will also produce a drag in the direction of flow, regardless of spin direction.

At the aircraft level, side forces exactly cancel on the cross-configuration quadcopter, but the plus-configuration quadcopter experiences a small net side force. Although the net side forces are small, since the aft rotor in the plus-configuration produces more thrust than the front rotor (to maintain the nose-down attitude), the aft rotor produces more side force, resulting in a net nose-right yawing moment (Fig. 12(a)). The cross-configuration, however, does not have a net yawing moment, as the two front rotors produce side forces of equal magnitude in opposing directions, as do the two aft rotors (Fig. 12(b)). This difference in the yawing moment directly leads to a difference in required yaw control, which is zero for the cross-configuration, and nonzero for the plus-configuration (Fig. 13). Additionally, the nonlinearity in the relationship between rotor RPM and rotor torque results in the pitch control causing a net yawing moment in the plus-configuration, though this effect is smaller than that due to side force. Rotor drag does not produce a net yawing moment because in both the case of the plus- and cross-configuration quadcopters, the yawing moment produced by a drag on a rotor on the left is countered by a drag of the same magnitude

on another rotor on the right of the longitudinal axis

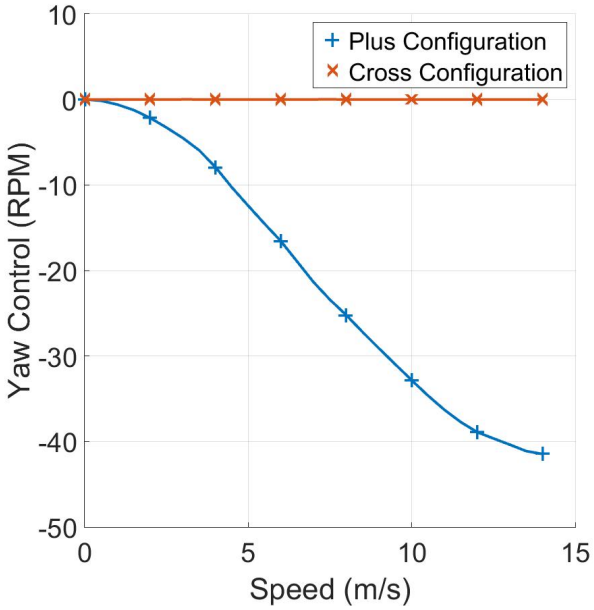

Fig. 13: Yaw Control versus Flight Speed

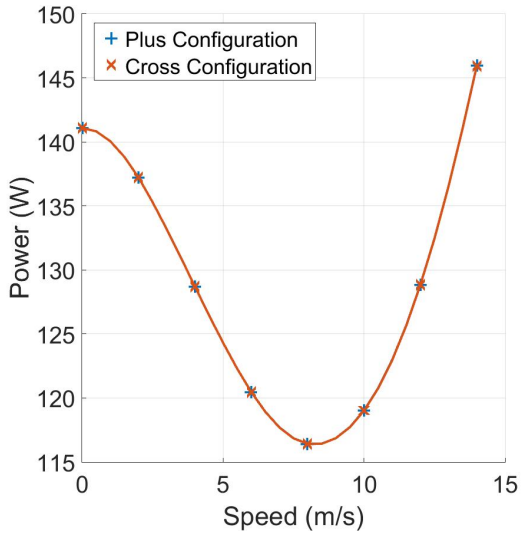

Fig. 14: Power Requirements for quadcopters

Despite these differences in the pitch and yaw trim controls between the plus and cross-configurations, the required power at all speeds is the same (Fig. 14). The reason for this is twofold. First, the power, generally cubic with the rotational speed, is dominated by the collective control requirements, which is generally much larger than the other controls. Second, although the cross-configuration requires less pitch control than the plus-configuration, it also applies pitch RPM to all of the rotors, so one unit of Ω_P is more costly on the plus-configuration than on the plus-configuration.

FLIGHT DYNAMICS RESULTS

The poles of the full system, linearized about the hover trim condition as in Eq. 4 are plotted in Fig. 15. As expected, the inflow states have very large negative real components, while the aircraft rigid body modes clustered relatively near the origin.

After the application of static condensation, the linear model takes the form of Eq. 6. Setting $\vec{u} = 0$ and taking the eigenvalues of $\bar{A}$, a set of reduced order poles corresponding to the aircraft rigid body modes are obtained. These poles and their locations are plotted against the full model rigid body poles in Fig. 16. The two sets of poles are very close to one another, validating the model reduction using static condensation.

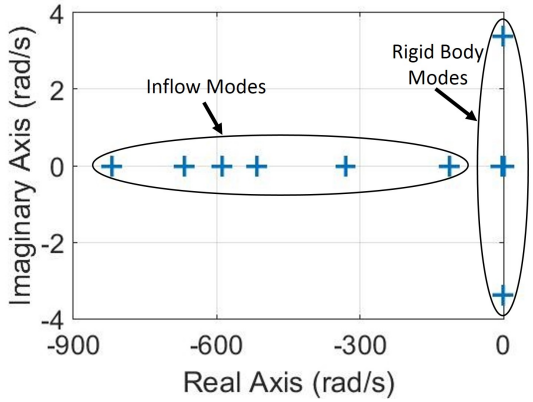

(a) Full Aircraft Poles

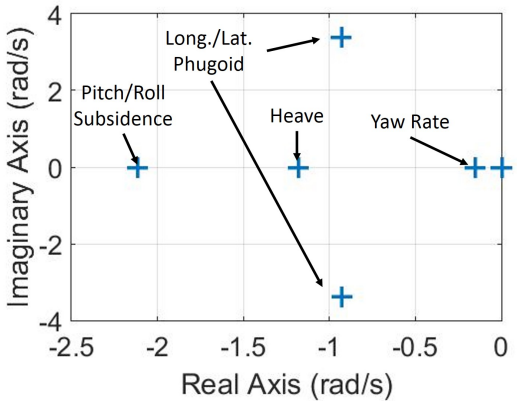

(b) Rigid Body Poles

Fig. 15: Locations of the poles of the quadcopter in hover (Plus configuration)

Hover

Each of the poles in Fig. 16 corresponds to a rigid body mode of the aircraft. Four of these poles at the origin are simple integrators, three of which correspond to the position of the aircraft, which has no effect on its behavior (ground effect and

atmospheric changes are not modeled). In hover, the heading also has zero effect on the dynamics of the aircraft.

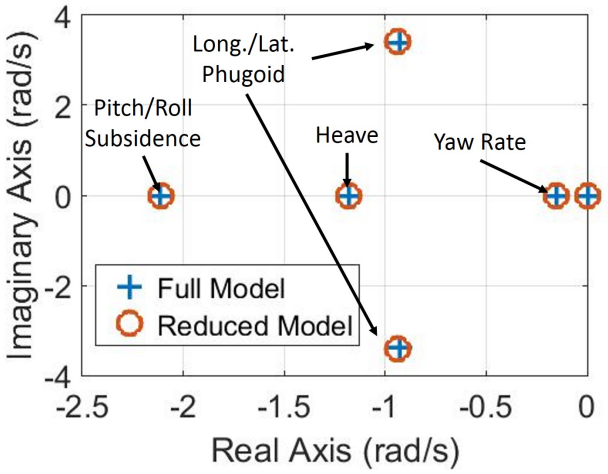

Fig. 16: Rigid body pole locations for full and reduced models (Plus configuration)

In addition to the integrators, there are four poles on the real axis in hover, all of which are stable. When the quadcopter's vertical velocity is perturbed, say in the upward direction, additional downwash over the rotors reduces their lift, causing a net reduction in lift. Since the aircraft began from a trimmed state, this causes a downward acceleration. Conversely, if the aircraft is perturbed in the downward direction, upwash increases rotor lift, causing an upward acceleration. Thus, this heave mode is well-damped.

Second, if the aircraft yaw rate is perturbed, each of the rotors begins traveling in plane. Aerodynamic drag acts on each rotor, producing a net yaw torque against the yaw perturbation (See Fig. 17). The remaining two real modes are a roll and pitch subsidence. Because the aircraft is symmetric, these two poles lie on top of one another in hover.

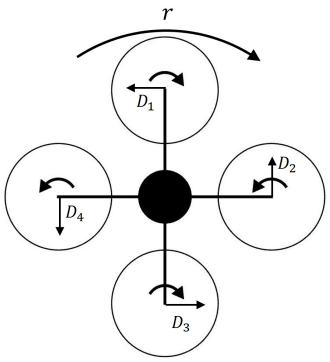

Fig. 17: Yaw Rate Mode

Finally, there are two pairs of complex conjugate poles, which correspond to a longitudinal and a lateral phugoid mode. The longitudinal phugoid mode begins with a nose-down pitch attitude (Fig. 18, (1)). This attitude causes the aircraft to begin traveling forward. As the aircraft travels forward, it begins to reorient nose-up due to the longitudinal thrust distribution on each rotor (Fig. 9) and due to a restoring moment caused by gravity, causing it to slow down (Fig. 18, 2–4). Eventually, it reaches a maximum nose-up attitude (Fig. 18, 5), and travels backward through 6–8, returning to 1. Although Fig. 18 depicts the return segment vertically offset from the forward segment, this is only done for clarity to show the different pitch attitudes between the two segments. There is also a lateral phugoid mode, which substitutes pitch for roll, and forward travel for sideward travel.

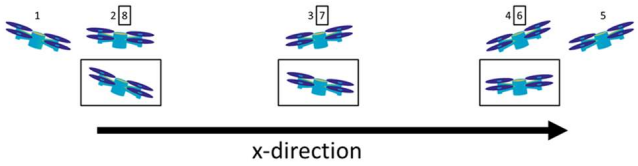

Fig. 18: Phugoid mode in hover, return segment offset vertically (shown in rectangular boxes)

The phugoid mode is governed by the longitudinal stability derivatives, namely X_θ, X_u, M_θ, and especially M_u, and M_q. M_u is a pitching moment derived from forward flight, which is created by the thrust distribution on the rotors (seen in Fig. 9). This moment, absent other forces, would cause the maximum pitch attitude at position 5 in Fig 18 to be greater than that at position 1, and then as it traveled back to 1, it would have an even greater pitch attitude. Thus, this moment destabilizes the system.

As the aircraft pitches, say nose-up, the front rotor(s) are forced upward through the air. This causes additional inflow over the entire rotor, which causes a corresponding decrease in thrust. Similarly, the aft rotor(s) are pushed down, causing an upwash and an increase in thrust. Taken together, the rotors produce a nose-down pitching moment. Conversely, as the aircraft pitched nose-down, a nose-up pitching moment is generated. Thus M_q is a damping term, and tends to stabilize the system.

M_θ is a moment produced by pitch attitude, and is generated by gravity (system reference point directly above the center of gravity), effecting a restoring moment and behaving as a stiffness term in the phugoid mode. The lower the center of gravity is relative to the reference point, the more stable the system will become. X_u is a drag term, and will tend to stabilize the phugoid mode. X_θ comes from the reorientation of thrust, and couples the pitch attitude to the translation.

The lateral phugoid mode is similarly governed by Y_ϕ, Y_v, L_ϕ, L_v, and L_p. In fact, in hover, the magnitudes of each component are exactly the same, that is $Y_\phi = -X_\theta$, $Y_v = X_u$, $L_\phi = M_\theta$, $L_v = -M_u$, and $L_p = M_q$. Sign differences are a result of the definition of the North-East-Down coordinate system.

Dynamic pole locations for reduced-order models on the plus and cross-configurations in hover are plotted in Fig. 19.

The poles are exactly the same, which is to be expected, since the quadcopter is heading-insensitive in hover.

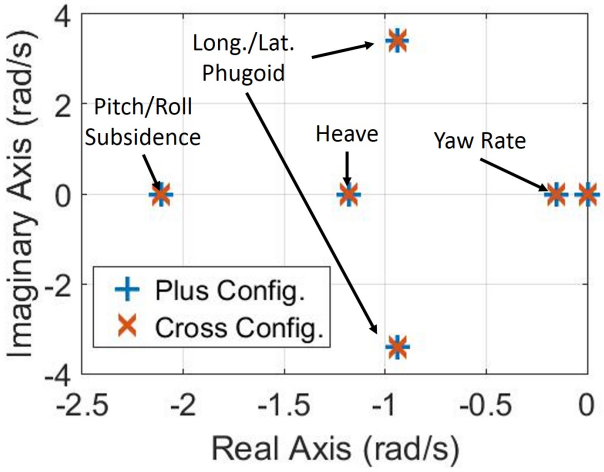

Fig. 19: Hover Poles of Plus and Cross Configuration

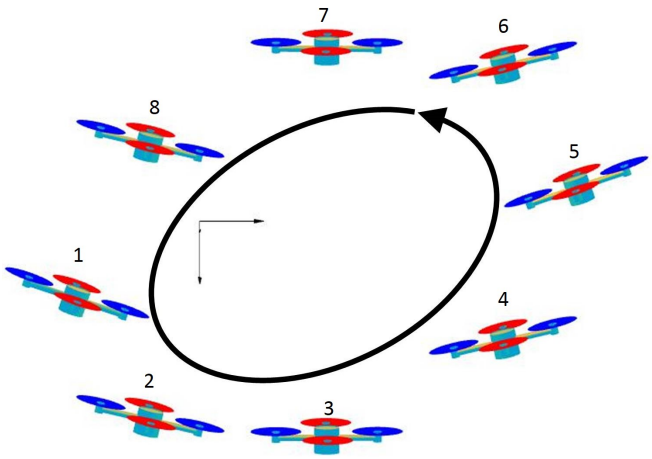

Fig. 21: Longitudinal phugoid mode in forward flight

Forward Flight

In forward flight, the two phugoid modes separate, becoming two distinct modes with distinct eigenvalues (Fig. 20). The damping ratio of the longitudinal phugoid mode generally increases with forward speed. That of the lateral phugoid mode remains mostly level until high speed is reached, where the damping increases sharply. The natural frequency of the longitudinal phugoid mode increases until it reaches a maximum at 7 m/s, where it levels off. The lateral phugoid mode frequency increases until it reaches a maximum at 9 m/s, and then decreases.

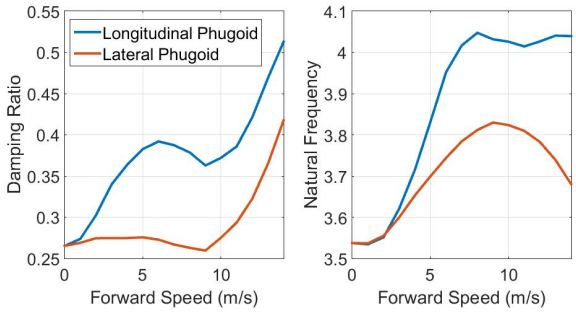

Fig. 20: Damping Ratio and Natural Frequency of the longitudinal and lateral phugoid modes in forward flight

The shape of the lateral phugoid mode in forward flight is very similar to hover, with lateral translation coupled to roll attitude, and nothing else. However, in forward flight, the longitudinal phugoid mode begins to include altitude changes. As the aircraft advances, it climbs, and as it retreats, it descends (Fig. 21).

Similar to the phugoid modes, the pitch and roll subsidence modes also split in forward flight. As the aircraft reaches moderate speeds, the pitch subsidence mode couples with the heave mode to form an oscillatory short-period mode. This mode is highly damped in all cases, and as forward speed increases, it becomes sufficiently damped to split back into a pitch subsidence and heave mode (Fig. 22).

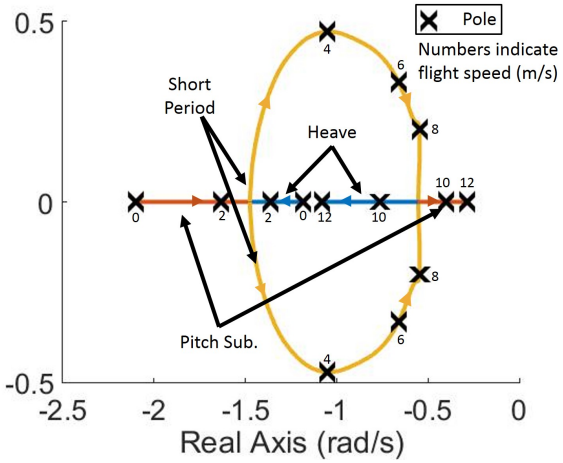

Fig. 22: Pitch Subsidence and Heave Modes

At any speed, the pole locations of the quadcopter are not impacted by the flight configuration (Fig. 23). Thus, the autonomous behavior of both the plus- and cross-configuration quadcopter is very similar in all steady flight conditions.

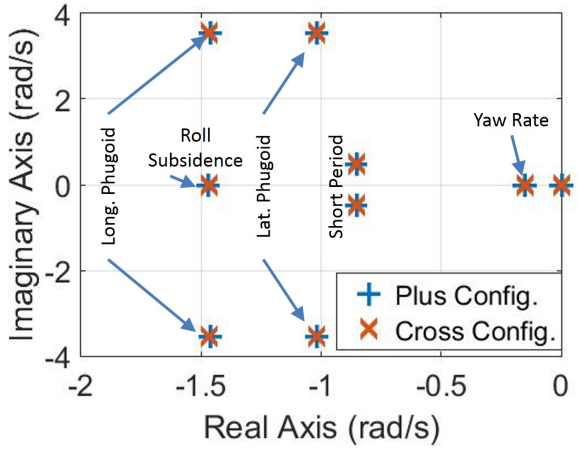

(a) Poles at 5 m/s

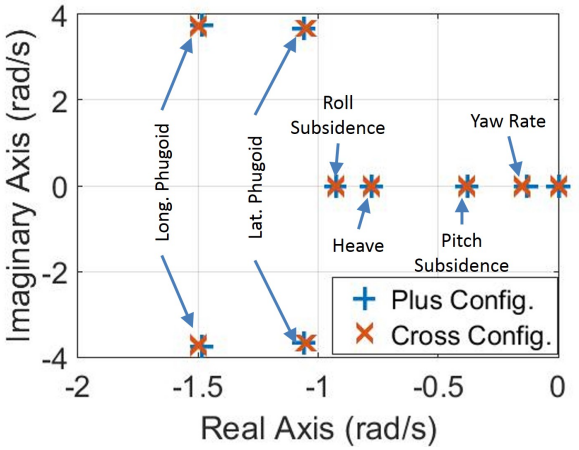

(b) Poles at 10 m/s

Fig. 23: Comparison of poles in forward flight

CONTROL AUTHORITY

Though there are no substantial differences between the plus and cross-configuration in the autonomous behavior of the aircraft, the two have different control schemes, and thus will have additional differences in their control sensitivities and authority. The control sensitivities are the entries of the matrix $\bar{B}$ in equation 6, which, in hover, takes the following form:

$$\bar{B} = \begin{bmatrix} 0 & 0 & 0 & 0 & 0 & 0 & 0 & 0 & Z_{\Omega_0} & 0 & 0 & 0 \\ 0 & 0 & 0 & 0 & 0 & 0 & 0 & 0 & 0 & 0 & M_{\Omega_P} & 0 \\ 0 & 0 & 0 & 0 & 0 & 0 & 0 & 0 & 0 & L_{\Omega_R} & 0 & 0 \\ 0 & 0 & 0 & 0 & 0 & 0 & 0 & 0 & 0 & 0 & 0 & N_{\Omega_Y} \end{bmatrix}^T$$

There is only one nonzero entry in each of the columns of $\bar{B}$, an advantage of the multi-rotor controls defined in Figs. 2 - 5. In forward flight, there will be other nonzero terms in $\bar{B}$, a consequence of the nonlinear rotor physics. Using a simplifying assumption on the rotor thrusts and torques (Eq. 7), we can obtain analytical estimates for the entries of $\bar{B}$ for each configuration.

$$T_i = a\Omega_i^2 \qquad \tau_i b\Omega_i^2 \tag{7}$$

where a and b are proportionality constants. All other forces and moments are assumed to be zero. The total forces and moments on the aircraft are given by equation 8.

$$\begin{aligned} T &= a\sum_{i=1}^{4}\Omega_i^2 & M &= -al\sum_{i=1}^{4}\Omega_i^2\cos\Psi_i \\ L &= -al\sum_{i=1}^{4}\Omega_i^2\sin\Psi_i & N &= -b\sum_{i=1}^{4}\Omega_i^2(-1)^i \end{aligned} \tag{8}$$

where l is the length of the boom attaching the rotor to the centerbody, and Ψ is an angle defined as zero on the aft of the quadcopter, and increasing counterclockwise looking downward at the aircraft. Consider first the thrust in the plus-configuration.

$$\Omega = \begin{bmatrix} \Omega_0 + \Omega_P + \Omega_Y \\ \Omega_0 + \Omega_R - \Omega_Y \\ \Omega_0 - \Omega_P + \Omega_Y \\ \Omega_0 - \Omega_R - \Omega_Y \end{bmatrix} \tag{9}$$

$$\begin{aligned} T &= a(\Omega_0+\Omega_P+\Omega_Y)^2 + a(\Omega_0+\Omega_R+\Omega_Y)^2 \\ &+ a(\Omega_0-\Omega_P+\Omega_Y)^2 + a(\Omega_0-\Omega_R+\Omega_Y)^2 \\ &= a(\Omega_0^2+\Omega_P^2+\Omega_Y^2+2\Omega_0\Omega_P+2\Omega_0\Omega_Y+2\Omega_P\Omega_Y) \\ &+ a(\Omega_0^2+\Omega_R^2+\Omega_Y^2+2\Omega_0\Omega_R-2\Omega_0\Omega_Y-2\Omega_R\Omega_Y) \\ &+ a(\Omega_0^2+\Omega_P^2+\Omega_Y^2-2\Omega_0\Omega_P+2\Omega_0\Omega_Y-2\Omega_P\Omega_Y) \\ &+ a(\Omega_0^2+\Omega_R^2+\Omega_Y^2-2\Omega_0\Omega_R-2\Omega_0\Omega_Y+2\Omega_R\Omega_Y) \\ &= a(4\Omega_0^2+2\Omega_P^2+2\Omega_R^2+4\Omega_Y^2) \\ &\approx 4a\Omega_0^2 \end{aligned} \tag{10}$$

where the assumption that $\Omega_0 >> \Omega_P, \Omega_R, \Omega_Y$, justified by Figs. 8, 10,. and 13, is applied. Taking the derivative with respect to Ω_0 yields an expression for Z_{Ω_0}.

$$Z_{\Omega_0} \propto \frac{\partial T}{\partial \Omega_0} = 8a\Omega_0 \tag{11}$$

with a proportionality constant equal to the inverse of the mass of the quadcopter. Applying the same analysis to the cross-type quadcopter will yield an equation identical to equation 11.

Next, consider the pitching moment on the plus-type quadcopter. Clearly, only the front and aft rotors will contribute.

$$\begin{aligned} M &= al(\Omega_0+\Omega_P+\Omega_Y)^2 - al(\Omega_0-\Omega_P+\Omega_Y)^2 \\ &= al(\Omega_0^2+\Omega_P^2+\Omega_Y^2+2\Omega_0\Omega_P+2\Omega_0\Omega_Y+2\Omega_P\Omega_Y) \\ &- al(\Omega_0^2+\Omega_P^2+\Omega_Y^2-2\Omega_0\Omega_P+2\Omega_0\Omega_Y-2\Omega_P\Omega_Y) \\ &= 4al\Omega_P(\Omega_0+\Omega_Y) \\ &\approx 4al\Omega_0\Omega_P \\ M_{\Omega_P} &\propto \frac{\partial M}{\partial \Omega_P} = 4al\Omega_0 \end{aligned} \tag{12}$$

with a proportionality constant equal to the inverse of the inertia of the quadcopter about the pitch axis. When applying the same analysis to the cross-type quadcopter, we must consider all four rotors, and also that they act at $\pm l \sin 45^\circ = l/\sqrt{2}$.

$$\begin{aligned} M &= \frac{al}{\sqrt{2}}(\Omega_0+\Omega_P-\Omega_R+\Omega_Y)^2+\frac{al}{\sqrt{2}}(\Omega_0+\Omega_P+\Omega_R-\Omega_Y)^2 \\ &\quad -\frac{al}{\sqrt{2}}(\Omega_0-\Omega_P+\Omega_R+\Omega_Y)^2-\frac{al}{\sqrt{2}}(\Omega_0-\Omega_P-\Omega_R-\Omega_Y)^2 \\ &= \frac{8al}{\sqrt{2}}(\Omega_0\Omega_P-\Omega_R\Omega_Y) \\ &\approx 4\sqrt{2}al\Omega_0\Omega_P \\ M_{\Omega_P} &\propto \frac{\partial M}{\partial \Omega_P} = 4\sqrt{2}al\Omega_0 \end{aligned} \tag{13}$$

with the same proportionality constant as in the plus case. Because the required collective control in any trim condition is identical for both quadcopter configurations (Fig. 8), we can conclude that the cross-type quadcopter should be more sensitive to pitch RPM input than the plus-type quadcopter by a factor of $\sqrt{2}$. The prediction of higher sensitivity is verified by Fig. 24, which shows the pitch control sensitivity from Eq. 6 of both quadcopter configurations versus forward flight.

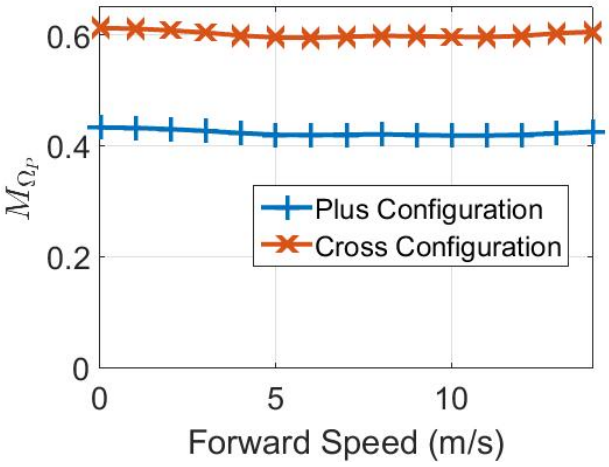

Fig. 24: Pitch RPM sensitivity of quadcopters

A similar analysis on the roll sensitivity yields

$$L_{\Omega_R} \propto \frac{\partial L}{\partial \Omega_R} = kal\Omega_0 \tag{14}$$

where $k = 4$ for the plus-type quadcopter, and $k = 4\sqrt{2}$ for the cross-type.

Finally, consider differential yaw. The rotors spinning counterclockwise (rotors N and S in Fig. 1(a) and rotors NE and SW in Fig. 1(b)) produce a nose-right (positive) reaction torque, while the rotors spinning clockwise (rotors E and W in Fig. 1(a) and rotors NW and SE in Fig. 1(b)). Summing the moments yields equation 15.

$$\begin{aligned} N &= b(\Omega_0+\Omega_P+\Omega_Y)^2-b(\Omega_0+\Omega_R-\Omega_Y)^2 \\ &\quad +b(\Omega_0-\Omega_P+\Omega_Y)^2-b(\Omega_0-\Omega_R-\Omega_Y)^2 \\ &= 2b(4\Omega_0\Omega_Y+\Omega_P^2+\Omega_R^2) \\ &\approx 8b\Omega_0\Omega_Y \\ N_{\Omega_Y} &\propto \frac{\partial N}{\partial \Omega_Y} = 8b\Omega_0 \end{aligned} \tag{15}$$

Once again, the proportionality constant is equal to the inverse of the inertia about the yaw axis. Analyzing the cross-type quadcopter will yield the same relationship.

Because these two configurations have the same inertias, the control authority will be defined by the maximum amount of moment that can be generated, which in turn will be determined by the maximum rotational speed of any given rotor $\Omega_{\max}$. Consider moments about the aircraft pitch axis in hover. To maintain hovering flight, both the plus and cross-configuration must apply the same $\Omega_0 < \Omega_{\max}$. When Ω_P is applied, the rotor with the highest speed (in both configurations) will rotate at $\Omega_0 + \Omega_P$. Thus, both configurations will maximize their pitching moment when $\Omega_P = \Omega_{\max} - \Omega_0$. However, since the sensitivities of pitching moment of the aircraft with respect to Ω_P are higher for the cross-type quadcopter, it will be able to produce more moment, and thus, will be more maneuverable about the pitch (and roll) axis in hover. However, this extra moment will come at the cost of greater power, since two rotors are used. Additionally, for larger pitching moments on the cross-type quadcopter, some roll authority will be sacrificed, as the rotor whose speed is increased by both the pitch and roll inputs will saturate at a lower rolling moment than if zero pitching input were applied. Whether this sacrifice in roll exceeds the gain in authority by using two rotors instead of one will depend on the applied pitching moment.

CONCLUSIONS

This paper compares a quadcopter operating in the plus and cross configurations. The mutli-rotor controls (collective, pitch, roll, and yaw control) are related to the individual rotor controls for each configuration. For a quadcopter in the plus configuration, pitch or roll control input generates a yaw moment, but for the cross-configuration, pitch and roll control is decoupled from yaw.

The studies in this paper model the quadcopter as a 6 degree-of-freedom rigid body and derive equations of motion by considering force and moment equilibrium about three axes. In addition to hub drag and gravity effects, the individual rotor forces are calculated using blade-element theory and a 3x4 (10 state) Peters-He dynamic wake model is used to represent the inflow variation for each rotor. A linearized model is derived for the flight dynamic studies and static condensation of the inflow states is used to reduce the problem size.

Based on trim studies over an airspeed range of 0-14 m/s, the quadcopter configuration does not affect the collective

controls, pitch attitude and power requirements. The pitch control requirement for a plus-configuration quadcopter is greater than the cross-configuration since the latter uses all four rotors to generate pitching moment as opposed to only two for the plus configuration. The plus-configuration quadcopter also requires a yaw control input in forward flight, which is not required for the cross-configuration.

An examination of the flight dynamic characteristics revealed that quadcopters display two oscillatory modes in hover, a longitudinal phugoid mode (coupling longitudinal translation and pitch) and a lateral phugoid mode (coupling lateral translation and roll). Both these modes are stable and their poles are coincident in hover. In forward flight, these modes separate, and the frequency and damping of both modes increases. The nature of the lateral phugoid mode in forward flight is very similar to hover, but the longitudinal phugoid mode begins to include altitude changes (in addition to longitudinal translation and pitch attitude). Over a certain airspeed range, a couple of real poles (corresponding to heave and pitch subsidence) combine to result in an oscillatory short-period mode. No significant difference is seen in the autonomous flight dynamic characteriscs (pole locations) are observed between the plus- and cross-configurations.

A comparison of the control authority available between the plus- and cross-configuration quadcopters shows that the collective and yaw control authority is identical, but the pitch and roll control authority is up to about 30% greater for the cross-configuration since all four rotors are used (as opposed to using only two for the plus configuration).

Author contact: Robert Niemiec, niemir@rpi.edu; Farhan Gandhi - Corresponding Author, fgandhi@rpi.edu

ACKNOWLEDGMENTS

This research was conducted with Government support under and awarded by DoD, Air Force Office of Scientific Research, National Defense Science and Engineering Graduate (NDSEG) Fellowship, 32 CFR 168a.

REFERENCES

[1]Pounds, P., Mahony, R., Hynes, P., and Roberts, J. "Design of a Four-Rotor Aerial Robot," 2002 Australasian Conference on Robotics and Automation, Auckland, New Zealand, November 27–29, 2002.

[2]Pounds, P., Mahony, R., Gresham, J., Corke, P., and Roberts, J. "Towards Dynamically Favourable Quad-Rotor Aerial Robots," 2004 Australasian Conference on Robotics and Automation, Canberra, Australia, December 6–8, 2004.

[3]Pounds, P., Mahony, R., and Corke, P., "Modelling and Control of a Quad-Rotor Robot" 2006 Australasian Conference on Robotics and Automation, Auckland, New Zealand, December 6–8, 2006.

[4]Pounds, P., and Mahony, R., "Design Principles of Large Quadrotors for Practical Applications," 2009 IEEE International Conference on Robotics and Automation, Kobe, Japan, May 12–17 2009.

[5]Haviland, S., Bershadsky, D., Magree, D., and Johnson, E., "Development of a 500 gram Vision-based Autonomous Quadrotor Vehicle Capable of Indoor Navigation," 71st Annual Forum of the American Helicopter Society International, Virginia Beach, Virginia, May 5–7, 2015

[6]Avera, M., Kand, M., and Singh, R., "Performance and Controllability Assessment of an Overlapping Quad-Rotor Concept," 72nd Annual Forum of the American Helicopter Society International, West Palm Beach, Florida, May 17–19, 2016.

[7]Hoffmann, G., Huang, H., Waslander, S., and Tomlin, C., "Quadrotor Flight Dynamics and Control: Theory and Experiment," 2007 AIAA Guidance, Navigation and Control Conference and Exhibit, Hilton Head, South Carolina, August 20–23, 2007.

[8]Huang, H., Hoffmann, G., Waslander, S., and Tomlin, C., "Aerodynamics and Control of Autonomous Quadrotor Helicopters in Aggressive Maneuvering," 2009 IEEE International Conference on Robotics and Automation, Kobe, Japan, May 12–17, 2009.

[9]Bouabdallah, S., and Seigwart, R., "Full Control of a Quadrotor," 2007 IEEE/RSJ International Conference on Intelligent Robots and Systems, San Diego, California, October 29–November 2, 2007.

[10]Erginer, B., and Altuğ, E, "Modeling and PD Control of a Quadrotor VTOL Vehicle," 2007 IEEE Intelligent Vehicles Symposium, Istanbul, Turkey, June 13–15, 2007.

[11]Mueller, M., D'Andrea, R., "Stability and Control of a Quadrocopter Despite the Complete Loss of One, Two, or Three Propellers," 2014 IEEE International Conference on Robotics and Automation, Hong Kong, China, May 31–June 7, 2014.

[12]Mulgaonkar, Y., Cross, G., Kumar, V., "Design of Small, Safe, and Robust Quadrotor Swarms," 2015 IEEE International Conference on Robotics and Automation, Seattle, Washington, May 26-30, 2015.

[13]Niemiec, R., Gandhi, F., "Effects of Inflow Model on Simulated Aeromechanics of Quadrotor Helicopters" 72nd Annual Forum of the American Helicopter Society International, West Palm Beach, Florida, May 17–19 2016.

[14]Peters, D., He, C., "A finite-state induced-flow model for rotors in hover and forward flight," 43rd Annual National Forum of the American Helicopter Society, St. Louis, MO, May 1987.